

COMPARISONS OF NUMERICAL AND EXPERIMENTAL EVALUATIONS OF VISCOELASTIC SANDWICH BEAMS

Waldir F. Filho and Flávio S. Barbosa

*Federal University of Juiz de Fora, Juiz de Fora, Brazil, Graduation Program in Computational
Modeling, waldir.filippe@gmail.com, flavio.barbosa@ufjf.edu.br*

Keywords: Structural dynamics, Viscoelastic Materials, GHM model, ADF model.

Abstract. The application of Viscoelastic Materials (VEM) as a passive or semi-active damping treatment has been shown as a good damping strategy. In order to design these damping treatments on actual problems, one should analyze at least two phases: firstly to estimate the mechanical properties of the applied VEM; and, secondly, to simulate the structural behavior by means of numerical and/or experimental tests.

In this paper, the results of two time domain based VEM numerical models are compared with experimental counterpart available in literature. Initially, the dynamic properties of the used VEMs are analyzed and, subsequently, the dissipative characteristics of this passive structural control are also evaluated.

1 INTRODUCTION

Aiming the reduction of structural vibrations, several techniques were developed to increase structural damping. Among these techniques, the passive control with viscoelastic materials has shown reasonable efficiency. These materials have low bearing properties with high dissipative capacity when subjected to cyclic deformations. That is the main reason that justifies the wide application of VEM in sandwich layers with stiff elastic materials working as a passive control system ([Felippe et al., 2013](#)). This type of control systems have experienced a growth in practical applications also due to some benefits related to cost-effectiveness ([Kim et al., 2006](#); [Battista et al., 2010](#); [Saidi et al., 2011](#); [Moliner et al., 2012](#)).

Computational modeling of VEM materials may be performed in frequency domain or in time domain. Due to mechanical properties frequency dependence of VEM, time domain based models are not as numerous as frequency domain methods. In view of facilities that time domain methods may directly provide, such as the maximum displacement range in a structural model analysis, many researchers have been developing numerical methods to simulate the dynamical response of VEM in time domain.

Among these time-domain based methods for VEM, those that introduce extra dissipation coordinates or internal variables in order to apply the Finite Element Method (FEM), has been applied in several situations such as the ones presented by [Wang et al. \(2000\)](#), [Roy et al. \(2008\)](#), [Friswell et al. \(2010\)](#) and [Wang and Inman \(2013\)](#). In this context, it is possible to observe that Golla-Hughes-McTavish (GHM) method ([Golla and Hughes, 1985](#); [McTavish and Hughes, 1993](#)) and Anelastic Displacement Field (ADF) method ([Lesieutre and Mingori, 1990](#); [Lesieutre, 1992](#); [Lesieutre and Bianchini, 1993](#); [Lesieutre and Govindswamy, 1996](#); [Lesieutre and Lee, 1996](#)) are a frequent choice to simulate the dynamic response of VEM.

In that way, this paper will discuss the computational modeling of VEM and their use for reducing vibrations in structures, working as passive control mechanism in sandwich layers. Computational viscoelastic sandwich models, based on GHM and ADF methods, are analyzed and their results are compared with theirs theoretical and experimental counterparts. Finally, an actual structure is used to evaluate the facilities and difficulties of each applied technique.

2 VISCOELASTIC MATERIALS MODELLING

2.1 The GHM Model

The stress-strain relation on Laplace's domain as mentioned by [Golla and Hughes \(1985\)](#) and [McTavish and Hughes \(1993\)](#) may be written as:

$$\sigma(s) = [E_0 + h(s)]\varepsilon(s), \quad (1)$$

where s is the Laplace operator, $\sigma(s)$ and $\varepsilon(s)$ are, respectively, the stress and strain on Laplace's domain, E_0 is the elastic fraction of complex modulus and $h(s)$ is the relaxation function. Function $h(s)$ can be written using Biot's series with four terms (or two GHM terms):

$$h(s) = \alpha_1 \frac{s^2 + \beta_1 s}{s^2 + \beta_1 s + \delta_1} + \alpha_2 \frac{s^2 + \beta_2 s}{s^2 + \beta_2 s + \delta_2}, \quad (2)$$

where N is the number of terms, α_i , β_i and δ_i are materials constants and $(\alpha_i, \beta_i, \delta_i) \geq 0$. Starting from the equation of motion in the Laplace domain:

$$\{Ms^2 + K\} q(s) = f(s), \quad (3)$$

being M , K and $f(s)$ respectively the mass, stiffness and external loading in the Laplace domain and:

$$K = \left[E_0 + \sum \alpha_i \right] K_v, \quad (4)$$

where: K_v is the rigidity fraction associated with geometrical characteristics of the model.

Therefore, the GHM model defines the equation of motion in the time domain as:

$$\begin{aligned} & \begin{bmatrix} M & 0 & 0 \\ 0 & \frac{\alpha_1}{\delta_1} K_v & 0 \\ 0 & 0 & \frac{\alpha_2}{\delta_2} K_v \end{bmatrix} \begin{Bmatrix} \ddot{q} \\ \ddot{\bar{z}}_1 \\ \ddot{\bar{z}}_2 \end{Bmatrix} + \begin{bmatrix} C & 0 & 0 \\ 0 & \frac{\alpha_1 \beta_1}{\delta_1} K_v & 0 \\ 0 & 0 & \frac{\alpha_2 \beta_2}{\delta_2} K_v \end{bmatrix} \begin{Bmatrix} \dot{q} \\ \ddot{\bar{z}}_1 \\ \ddot{\bar{z}}_2 \end{Bmatrix} \\ & + \begin{bmatrix} K_v(E_0 + \alpha_1 + \alpha_2) & -\alpha_1 K_v & -\alpha_2 K_v \\ -\alpha_1 K_v & K_v & 0 \\ -\alpha_2 K_v & 0 & K_v \end{bmatrix} \begin{Bmatrix} q \\ \bar{z}_1 \\ \bar{z}_2 \end{Bmatrix} = \begin{Bmatrix} f(t) \\ 0 \\ 0 \end{Bmatrix}, \quad (5) \end{aligned}$$

where z_i is the auxiliary variable introduced into the problem, called dissipation variable. Generalizing Equation (5) for n degrees of freedom, Equation (6) may be written as:

$$\begin{aligned} & \begin{bmatrix} M & 0 & 0 \\ 0 & \frac{\alpha_1}{\delta_1} I & 0 \\ I & I & \frac{\alpha_2}{\delta_2} I \end{bmatrix} \begin{Bmatrix} \ddot{\mathbf{q}} \\ \ddot{\mathbf{\bar{z}}}_1 \\ \ddot{\mathbf{\bar{z}}}_2 \end{Bmatrix} + \begin{bmatrix} 0 & 0 & 0 \\ 0 & \frac{\alpha_1 \beta_1}{\delta_1} I & 0 \\ 0 & 0 & \frac{\alpha_2 \beta_2}{\delta_2} I \end{bmatrix} \begin{Bmatrix} \dot{\mathbf{q}} \\ \dot{\mathbf{\bar{z}}}_1 \\ \dot{\mathbf{\bar{z}}}_2 \end{Bmatrix} \\ & + \begin{bmatrix} \mathbf{K}_v(E_0 + \sum \alpha_i) & -\alpha_1 \mathbf{R} & -\alpha_2 \mathbf{R} \\ -\alpha_1 \mathbf{R}^T & \alpha_1 I & 0 \\ -\alpha_2 \mathbf{R}^T & 0 & \alpha_2 I \end{bmatrix} \begin{Bmatrix} \mathbf{q} \\ \mathbf{\bar{z}}_1 \\ \mathbf{\bar{z}}_2 \end{Bmatrix} = \begin{Bmatrix} \mathbf{f}(t) \\ 0 \\ 0 \end{Bmatrix}, \quad (6) \end{aligned}$$

where: \mathbf{M} is the mass matrix of the corresponding elastic element,

$$\mathbf{K}_v = \mathbf{T}^T \Lambda \mathbf{T}, \quad (7)$$

and Λ is a diagonal matrix consisting of the non-zero eigen-values of the stiffness matrix normalized with respect to the elastic modulus, E ; \mathbf{T} is the matrix of eigen-vectors corresponding to the non-zero eigen-values of the matrix $(1/E)K_{elastic}$; $\mathbf{R} = \mathbf{T} \Lambda^{1/2}$ and $\mathbf{z}_i = \mathbf{R} \bar{\mathbf{z}}_i$. As shown in Equations (6) and (7) the number of dissipative degrees of freedom associated with viscoelastic elements depends on the number of terms used in relaxation function and the number of rigid body motions (Barbosa, 2000). It should be noted that the greater number of terms used to write function relaxation more accurate the model will be.

2.2 The ADF Model

Lesieutre (Lesieutre and Mingori, 1990) establishes that the displacement field can be written as:

$$q(t) = q^e(t) + \sum_{j=1}^N q_j^a(t), \quad (8)$$

where $q^e(t)$ is the elastic displacement field and $q_j^a(t)$ is the $j - th$ anelastic displacement field, then the strain field is defined as:

$$\varepsilon(t) = \varepsilon^e(t) + \sum_{j=1}^N \varepsilon_j^a(t). \quad (9)$$

The ADF model defines the equation of motion in time domain as:

$$M\ddot{q}(t) + \sigma(t) = f(t), \quad (10)$$

where $\sigma(t) = E^\infty \varepsilon^e(t)$ is the stress in material and E^∞ is the elastic modulus at high frequency. Considering Equations (9) and (10) one can write:

$$M\ddot{q}(t) + E^\infty \left(\varepsilon(t) - \sum_{j=1}^N \varepsilon_j^a(t) \right) = f(t). \quad (11)$$

Defining the anelastic stress as an “thermodynamic force” that carry the anelastic deformations to an equilibrium point, [Lesieutre and Mingori \(1990\)](#) defines the “relaxation equation” governing the time evolution of the anelastic displacement field as:

$$\frac{1}{\Omega_j} E_j^a \frac{\partial}{\partial t} \varepsilon_j^a(t) + E_j^a \varepsilon_j^a(t) - E^\infty \varepsilon(t) = 0 \quad (12)$$

being E_j^a the $j - th$ anelastic modulus and Ω_j is a material parameter. Applying the Finite Element Method on Equations (11) and (12) and considering just two terms on Equation (8) one can write:

$$\begin{bmatrix} \mathbf{M} & \mathbf{0} & \mathbf{0} \\ \mathbf{0} & \mathbf{0} & \mathbf{0} \\ \mathbf{I} & \mathbf{I} & \mathbf{0} \end{bmatrix} \begin{Bmatrix} \ddot{\mathbf{q}} \\ \ddot{\mathbf{q}}_1^a \\ \ddot{\mathbf{q}}_2^a \end{Bmatrix} + \begin{bmatrix} \mathbf{0} & \mathbf{0} & \mathbf{0} \\ \mathbf{0} & \frac{C_1}{\Omega_1} E^\infty \Lambda & \mathbf{0} \\ \mathbf{0} & \mathbf{0} & \frac{C_2}{\Omega_2} E^\infty \Lambda \end{bmatrix} \begin{Bmatrix} \dot{\mathbf{q}} \\ \dot{\mathbf{q}}_1^a \\ \dot{\mathbf{q}}_2^a \end{Bmatrix} + \begin{bmatrix} \mathbf{K}_v & -\mathbf{K}_v \mathbf{T} & -\mathbf{K}_v \mathbf{T} \\ -\mathbf{T} \mathbf{K}_v^T & C_1 E^\infty \Lambda & \mathbf{0} \\ -\mathbf{T} \mathbf{K}_v^T & \mathbf{0} & C_2 E^\infty \Lambda \end{bmatrix} \begin{Bmatrix} \mathbf{q} \\ \mathbf{q}_1^a \\ \mathbf{q}_2^a \end{Bmatrix} = \begin{Bmatrix} \mathbf{f}(t) \\ \mathbf{0} \\ \mathbf{0} \end{Bmatrix}, \quad (13)$$

where C_j is a material parameter defined by:

$$C_j = \frac{E_j^a}{E^\infty} = \frac{1 + \sum_{j=1}^N \Delta_j}{\Delta_j} \quad (14)$$

with Δ_j being another material parameter and, as in GHM Model, $\mathbf{K}_v = \mathbf{T}^T \boldsymbol{\Lambda} \mathbf{T}$.

As shown in Equations (8) and (13), the same observations about the number of dissipative degrees of freedom associated with viscoelastic elements can be made as the ones made for GHM model.

2.3 Validation of the VEM models

The validation test, applied in both methods, consists in evaluate the dynamic behavior of a viscoelastic cantilever beam. The beam has 1000mm length and rectangular cross section, 300mm height and 150mm width.

Numerical simulations were performed using FEM meshes of Constant Strain Triangular elements (CST) to discretize the domain of the structures. FEM matrices were achieved by means of Equations (6) and (13) for GHM and ADF methods, respectively.

In order to obtain the suitable refined mesh, a convergence analysis was performed until no significant difference in terms of displacements was observed for two levels of refinement. Once defined the configuration of the FEM mesh for each tested beam model, this mesh was used for the both formulations - GHM and ADF. The adopted mesh has 602,302 physical dof and 1,800,000 dissipative dof, 2,402,302 dof total. A schema of the used mesh is presented in Figure 1.

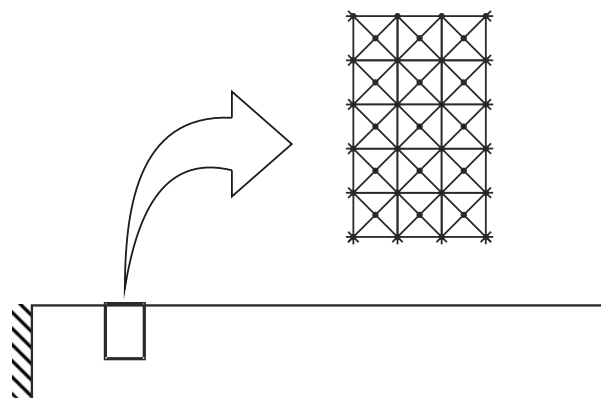


Figure 1: Structural Finite Element discretization for validation tests.

In order to better evaluate the accuracy of the analyzed methods, two VEM were used. For GHM and ADF tests, materials 1 and 2, respectively, were applied. Tables 1 and 2 presents the parameters of these materials used in Equations (6) and (13) to obtain the VEM cantilever models. This strategy was adopted due to differences at complex modulus expressions used on both formulations.

Parameter	Term 1	Term 2
E_0	637×10^6	
α	763774.0×10^6	763774.0×10^6
β	2.9178×10^7	2.9178×10^7
δ	3.2408×10^8	3.2408×10^8

Table 1: Material 1 parameters used in validation tests (GHM model).

GHM and ADF formulations allow time domain equations for VEM. However, using theirs respective frequency domain equations, it is possible to apply classical discrete solutions to compare and evaluate the quality of GHM and ADF results, as is explained bellow.

Starting from the dynamic equilibrium equations, using the complex excitation one has the classical discrete Equation (15):

$$\mathbf{M}\ddot{\mathbf{q}} + \mathbf{K}(\omega)\mathbf{q} = \mathbf{P} \exp(i\omega t), \quad (15)$$

Parameter	Term 1	Term 2
E_0	637×10^6	
Δ_j	2.0118	2.0118
Ω_j	83.0916	83.0916

Table 2: Material 2 parameters used in validation tests (ADF model).

where \mathbf{M} is the mass matrix of the structure; $\mathbf{K}(\omega)$ is the frequency dependent stiffness matrix of the structure; $\mathbf{P}_{exp}(i\omega t)$ is the harmonic excitation vector having ω as the excitation frequency and $i = \sqrt{-1}$. It can be noticed that if the mechanical properties of the structure is not frequency dependent, then $\mathbf{K}(\omega) = \mathbf{K}$ which is not the case of VEM.

Using GHM or ADF, Equation (15) may be rewritten as:

$$\bar{\mathbf{M}} \begin{Bmatrix} \ddot{\mathbf{q}} \\ \ddot{\mathbf{z}} \end{Bmatrix} + \bar{\mathbf{C}} \begin{Bmatrix} \dot{\mathbf{q}} \\ \dot{\mathbf{z}} \end{Bmatrix} + \bar{\mathbf{K}} \begin{Bmatrix} \mathbf{q} \\ \mathbf{z} \end{Bmatrix} = \begin{Bmatrix} \mathbf{P}_{exp}(i\omega t) \\ \mathbf{0} \end{Bmatrix}, \quad (16)$$

where $\bar{\mathbf{M}}$, $\bar{\mathbf{C}}$, $\bar{\mathbf{K}}$ are, respectively, the mass, damping and stiffness matrices, \mathbf{q} and \mathbf{z} are the displacement and dissipation variable vectors for GHM or ADF model. It is important to notice that the stiffness matrices in the GHM or ADF formulations are not frequency dependent.

The frequency domain displacements \mathbf{q} may be obtained by solving Equations (15) and (16), resulting in Equations (17) and (18), respectively:

$$\mathbf{q} = [\mathbf{K}(\omega) - \omega^2 \mathbf{M}]^{-1} \mathbf{P}, \quad (17)$$

$$\begin{Bmatrix} \mathbf{q} \\ \mathbf{z} \end{Bmatrix} = [\bar{\mathbf{K}}(\omega) + i\omega \bar{\mathbf{C}} - \omega^2 \bar{\mathbf{M}}]^{-1} \begin{Bmatrix} \mathbf{P} \\ \mathbf{0} \end{Bmatrix}. \quad (18)$$

By solving Equations (17) and (18) for the two beam models, Figure 2 may be achieved. It is possible to observe that, for all tested beam models, ADF and GHM formulations allow identical results when compared to the respective classical responses, supporting the accuracy of applied methods. These figures were achieved observing the vertical nodal displacements at the free end of the beam models, with only one nodal harmonic transversal load also at the free end. As it can be observed, both models produce de same response on frequency domain, as the classic formulation (Equation (17)).

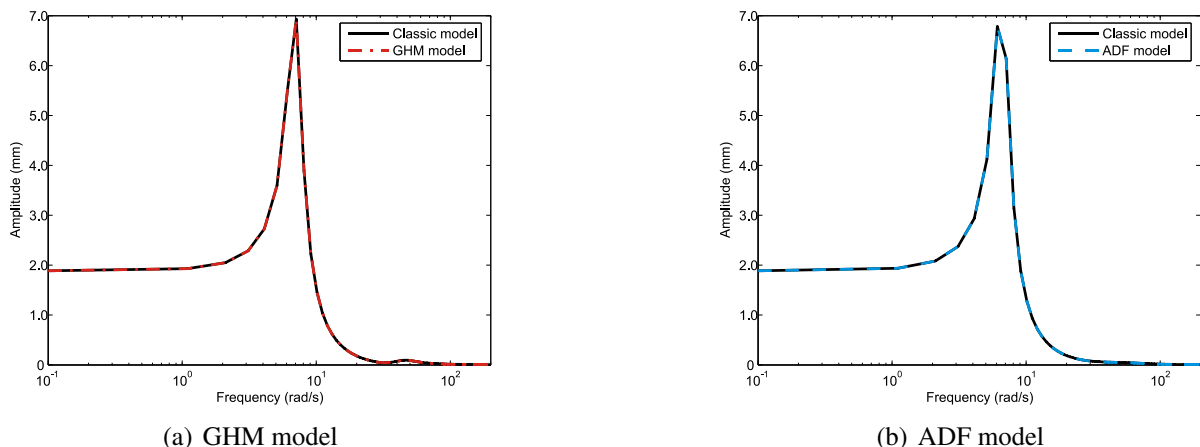


Figure 2: Frequency response for validation tests.

2.4 Time processing evaluation of numerical methods

Another parameter to compare both models is the time spent to numerical simulate models. Thereunto, both methods were implemented in MATLAB using the toolbox for sparse matrixes.

The used computer was an Intel Core 2 Duo computer with 2.1GHz clock and 2.00Gb RAM. The VEM cantilever beam models were evaluated 20 times, running under a Windows Vista Operational System. It was registered the total time spent to calculate the elementary matrices, assembly the global matrices and impose the boundary conditions. The elapsed time for solving the time integration problem was not taken into account since the involved global matrices of both methods have the same order resulting in practically the same integration time.

For the GHM model the mean processing time was 8.97h with standard deviation 1.83h; For ADF model the mean processing time was 8.00h with standard deviation 0.79. One can notice that the mean times of both models are close but the ADF model was slightly faster than GHM formulation and presented a smaller standard deviation ratio.

3 EXPERIMENTAL EVALUATION OF VEM STRUCTURES AND MATERIAL

3.1 Experimental program

In order to evaluate the viscoelastic models, experimental data was taken from literature. Borges (2010) performed a wide laboratory study. In these laboratory studies, a set of four kinds of sandwich beams were tested. The beams were grouped in accordance with its layer configuration:

1. **VS1 beam**, with two elastic layers (base beam and clamped restraining layer) and one viscoelastic layer;
2. **VS1c beam**, with two elastic layers (base beam and free restraining layer) and one viscoelastic layer;
3. **VS2 beam**, with three elastic layers (one base beam and two clamped restraining layers)and;
4. **VS2c beam**, with three elastic layers (one base beam and two free restraining layers).

The layer configurations of each sandwich beam group can be seen in Figure 3.

All beams have rectangular cross section and 1140 mm length; the bean working as elastic base structure has 16,1mm height; viscoelastic layers has 2,0mm height; and elastic constraining layers has 3,17mm height. The elastic material was aluminium and the viscoelastic material used was VHB 4955. Some mechanical properties of the materials are listed in Table 3.

Propertie	Aluminium	VHB 4955
E (GPa)	48.878	-
ν	0.30	0.49
ρ (kg/m^3)	2690.0	795.0

Table 3: Mechanical properties of beam materials.

Two geometrically identical base structures (base beam A and B) were used for each group of beams. This strategy was applied in order to evaluate the experimental result dispersion. It is

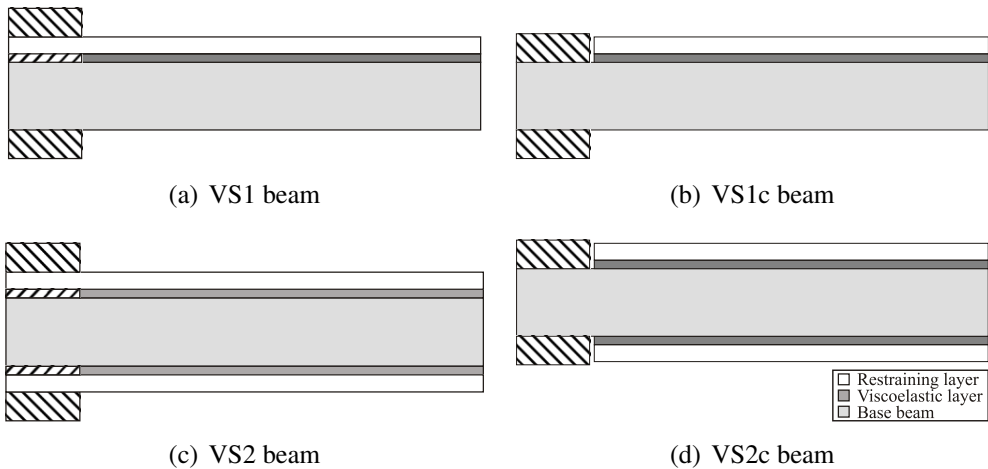


Figure 3: Longitudinal section of the analyzed beams.

Vib. Mode	Base beam A		Base beam B	
	Natural frequency (Hz)	Damping rate (%)	Natural frequency (Hz)	Damping rate (%)
1	10.25 ± 0.00	0.05 ± 0.00	10.24 ± 0.00	0.05 ± 0.00
2	63.38 ± 0.00	0.02 ± 0.00	63.70 ± 0.00	0.04 ± 0.00
3	179.00 ± 0.00	0.06 ± 0.00	179.26 ± 0.00	0.05 ± 0.00

Table 4: Natural frequencies and damping rates of base beams.

important to notice that damping ratio of the base beams A and B (without the viscoelastic core) were measured and in all analyzed cases they were close to zero as shown in Table 4.

The beams were excited under the action of a hammer impact at 15 cm from cantilever and at the same section the transversal displacements were measured .

3.2 VEM characterization

Table 5 present the results of VEM characterization test in terms of Shear Modulus, $G'(\omega)$, and Loss Factor, $\eta(\omega)$, for frequencies between 0 and 179 Hz.,

Frequency (Hz)	$G'(\omega)$ (MPa)	$\eta(\omega)$ (-)
11.17	0.895 ± 0.025	0.629 ± 0.047
62.58	1.204 ± 0.050	0.801 ± 0.094
171.88	2.468 ± 0.116	0.808 ± 0.249

Table 5: VHB 4955 characterization data. (Adapted from (Borges, 2010))

After the values of Complex Modulus are experimentally determined, one can adjust the curves of the real part of the Complex Modulus and the loss factor for the points obtained experimentally.

In the case of the GHM formulation, they are given, in terms of Shear Modulus, by:

$$G'(\omega) = G_0 + \sum_{j=1}^2 \alpha_j \frac{\omega^2(\omega^2 - \delta_j + \beta_j^2)}{(\delta_j - \omega^2)^2 + \beta_j^2 \omega^2}, \quad (19)$$

$$\eta(\omega) = \frac{1}{G'(\omega)} + \sum_{j=1}^2 \frac{\alpha_j \beta_j \delta_j \omega}{(\delta_j - \omega^2)^2 + \beta_j^2 \omega^2}, \quad (20)$$

and in the case of the ADF formulation these equations are:

$$G'(\omega) = G_0 \left(1 + \sum_{j=1}^2 C_j \frac{(\omega/\Omega_j)^2}{1 + (\omega/\Omega_j)^2} \right), \quad (21)$$

$$\eta(\omega) = \frac{\sum_{j=1}^2 C_j \frac{(\omega/\Omega_j)}{1 + (\omega/\Omega_j)^2}}{1 + \sum_{j=1}^2 C_j \frac{(\omega/\Omega_j)^2}{1 + (\omega/\Omega_j)^2}}, \quad (22)$$

Equations from (19) to (22) were used to determine the GHM and ADF materials parameters. In this work, it was applied a Particle Swarm Optimization (PSO) algorithm (DeJong, 1975) in order to curve fit the characterization equations. Using the data from the experiments between 0 and 179 Hz, the material parameters could be determined. These fitted values, defined in terms of Young Modulus, are shown in Table 6, for the GHM Model, and in Table 7, for the ADF Model. Figure 4 shows two graphics comparing the experimental values and the adjusted curves of $G'(\omega)$ and $\eta(\omega)$.

Parameter	Term 1	Term 2
E_0	3.7337×10^5	
α_j	7.5785×10^6	9.3972×10^5
β_j	5.9225×10^6	8.9636×10^7
δ_j	6.7544×10^9	4.2422×10^9

Table 6: GHM parameters adjusted to the viscoelastic material.

Parameter	Term 1	Term 2
E_0	4.7375×10^5	
Δ_j	5.8132	1.6795
Ω_j	400	13.2280

Table 7: ADF parameters adjusted to the viscoelastic material.

4 NUMERICAL EVALUATION

In order to numerically simulate the dynamical behavior of the beams, the structures were discretized with CST meshes as the one shown in Figure 5. These meshes had 98,084 physical dof and 54,720 dissipation dof (152,804 in total) for VS1 and VS1c beams and; 120,894 physical dof and 109,440 dissipation dof (230,334 in total) for VS2 and VS2c beams.

The models were simulated under the action of a hammer impact at 15 cm from cantilever and, at same point, it was observed the transversal displacement along the time. With the models given by Equations (6) and (13), the time response of the beams could be obtained.

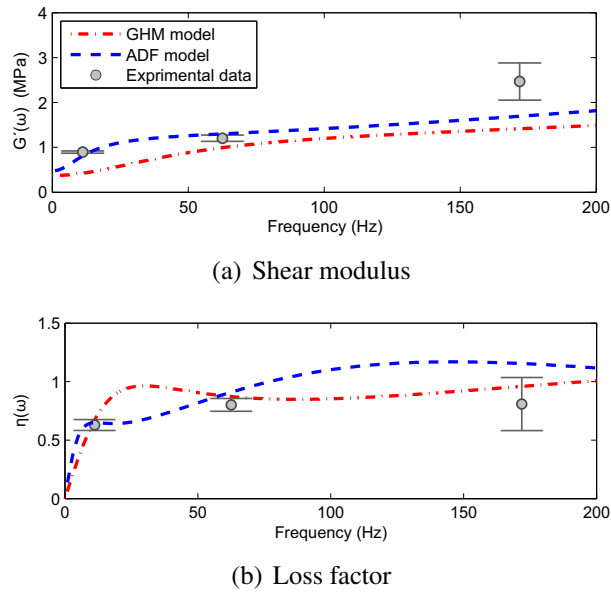


Figure 4: Experimental values and fitted curves of $G'(\omega)$ and $\eta(\omega)$.

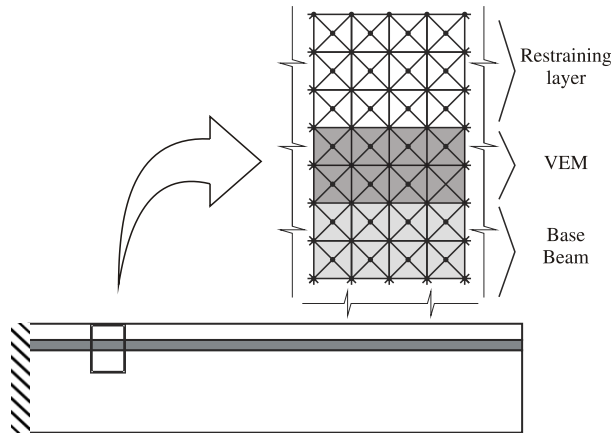


Figure 5: Viscoelastic sandwich cantilever beam structural Finite Element discretization.

Natural frequencies and damping ratios were extracted by means of an automatic Stochastic Subspace Identification algorithm as proposed by [Cabboi et al. \(2013\)](#).

5 RESULTS

For the four analyzed sandwich beams, natural frequencies and damping ratios experimentally and numerically obtained are listed in Tables 8, 9, 10 and 11. Experimental results for VS2 with base beam A were not presented by [Borges \(2010\)](#).

Vib. Mode	Experimental				Numerical			
	Base beam A		Base beam B		GHM		ADF	
	F_i (Hz)	ξ_i (%)	F_i (Hz)	ξ_i (%)	F_i (Hz)	ξ_i (%)	F_i (Hz)	ξ_i (%)
1	11.31	4.98	11.03	4.44	10.81	4.79	10.89	3.05
2	63.37	4.90	61.76	4.32	62.61	4.62	62.64	2.80
3	175.05	4.39	168.08	3.28	159.81	1.90	158.10	0.51

Table 8: Natural frequencies and damping ratios for beam VS1.

Vib. Mode	Experimental				Numerical			
	Base beam A		Base beam B		GHM		ADF	
	F_i (Hz)	ξ_i (%)	F_i (Hz)	ξ_i (%)	F_i (Hz)	ξ_i (%)	F_i (Hz)	ξ_i (%)
1	9.82	2.74	8.41	2.23	9.72	1.80	9.75	1.06
2	63.70	4.80	55.09	3.48	62.37	3.79	62.49	1.82
3	174.05	4.44	145.16	3.86	159.86	2.73	157.42	0.81

Table 9: Natural frequencies and damping ratios for beam VS1c.

Vib. Mode	Experimental				Numerical			
	Base beam A		Base beam B		GHM		ADF	
	F_i (Hz)	ξ_i (%)	F_i (Hz)	ξ_i (%)	F_i (Hz)	ξ_i (%)	F_i (Hz)	ξ_i (%)
1	-	-	12.34	7.92	11.43	7.99	11.46	4.91
2	-	-	64.79	8.65	62.15	6.91	62.38	3.81
3	-	-	173.29	6.17	157.62	4.01	154.67	1.15

Table 10: Natural frequencies and damping ratios for beam VS2.

Vib. Mode	Experimental				Numerical			
	Base beam A		Base beam B		GHM		ADF	
	F_i (Hz)	ξ_i (%)	F_i (Hz)	ξ_i (%)	F_i (Hz)	ξ_i (%)	F_i (Hz)	ξ_i (%)
1	8.26	4.75	9.82	5.14	9.32	3.18	9.41	1.92
2	56.81	6.67	65.43	8.60	61.94	7.24	61.94	3.70
3	146.04	4.73	172.33	5.90	156.65	4.03	153.48	1.36

Table 11: Natural frequencies and damping ratios for beam VS2c.

6 DISCUSSIONS AND CONCLUSIONS

This study evaluated the GHM and ADF methods on computational modeling of viscoelastic materials acting as structural sandwich dampers. Based on experimental data available in literature, it was shown that this type of passive control significantly improve the damping rates, since the damping contribution of the elastic beams were close to zero and, after the damper treatment, the sandwich beams achieved significant values for damping ratio as shown in Tables 8 to 11.

As one can observe, beams with clamped restraining layers (VS1c and VS2c) present higher damping rate than those without clamped restraining layers. This behavior was expected since beams with clamped restraining layers impose larger shear deformations on VEM. Consequently, the material dissipates more energy.

The GHM and ADF models were implemented in a finite element code and it was observed that both methods have excellent agreement when the results are compared to the respective classical frequency domain response.

By comparing the obtained responses with the experimentally tested beams, it is possible to notice that numerical natural frequencies have good agreement with the experimental counterpart for all tested beams.

Concerning damping ratios, GHM and ADF models tend to under-evaluate ξ values specially for higher frequencies. For ADF models this feature is more pronounced. Despite this, GHM results achieve fair results for damping ratios for a significant number of mode shapes.

With regards to time of processing, ADF was around 10% faster than GHM.

In view of the above, and taking into consideration the small difference in terms of performance between the analyzed methods and also the superior accuracy of GHM, authors suggest that GHM produces slightly better results than ADF models.

ACKNOWLEDGEMENTS Authors would like to thank: CNPq (Conselho Nacional de Desenvolvimento Científico e Tecnológico); UFJF (Federal University of Juiz de Fora); FAPEMIG (Fundação de Amparo à Pesquisa do Estado de Minas Gerais) and CAPES (Coordenação de Aperfeiçoamento de Pessoal de Nível Superior) for financial supports.

REFERENCES

- Barbosa F.S. *Modelagem computacional de estruturas com camadas viscoelásticas amortecedoras*. Phd thesis, COPPE/UFRJ, Rio de Janeiro, Brazil, 2000.
- Battista R.C., Santos E.F., Vasconcelos R., and Pfeil M.S. A visco-elastic sandwich solution for orthotropic decks of steel bridges. In *SDSS'Rio 2010 - Stability and ductility of steel structures*. 2010.
- Borges F.C. *Análise do comportamento dinâmico de vigas sanduíche com múltiplas camadas*. M.sc. thesis, COPPE/UFRJ, Rio de Janeiro, Brasil, 2010.
- Cabboi A., Magalhaes F., genile C., and Cunha A. Automatic operational modal analysis: Challenges and practical application to a historical bridge. *Proceedings of 6th ECCOMAS Conference on Smart Structures and Materials - SMART2013*, 2013.
- DeJong K. *An analysis of the behavior of a class of genetic adaptive systems*. Ph.d. thesis, University of Michigan, 1975.
- Felippe W., Barbosa F., Roitman N., Magluta C., and Borges F. Experimental and numerical

- evaluation of sandwich viscoelastic beams. *Proc., Experimental Vibration Analysis for Civil Engineering Structures - EVACES*, 2013.
- Friswell M., Dutt J., Adhikari S., and Lee. Time domain analysis of a viscoelastic rotor using internal variable models. *International Journal of Mechanical Sciences*, 52:1319–1324, 2010.
- Golla D. and Hughes P. Dynamics of viscoelastic structures - a time-domain, finite element formulation. *Journal of Applied Mechanics*, 52:897–906, 1985.
- Kim J., Ryu J., and Lan C. Seismic performance of structures connected by viscoelastic dampers. *Engineering Structures*, 28, 2006.
- Lesieutre G. Finite elements for dynamic modeling of uniaxial rods with frequency dependent material properties. *International Journal of Solids and Structures*, 29:1567–1579, 1992.
- Lesieutre G. and Bianchini E. Time domain modeling of linear viscoelasticity using anelastic displacement fields. *Journal of Vibration Acoustical*, 117:424–430, 1993.
- Lesieutre G. and Govindswamy K. Finite element modeling of frequency-dependent and temperature-dependent dynamic behavior of viscoelastic material in simple shear. *International Journal of Solids and Structures*, 33:419–432, 1996.
- Lesieutre G. and Lee U. A finite element for beams having segmented active constrained layers with frequency-dependent viscoelastics. *Smart Materials and Structures*, 5, 1996.
- Lesieutre G. and Mingori D. Finite element modeling of frequency-dependent materials properties using augmented thermodynamics fields. *Journal of Guidance Control and Dynamics*, 13:1040–1050, 1990.
- McTavish D. and Hughes P. Modeling of linear viscoelastic space structures. *Journal of Vibration and Acoustics*, 115:103–113, 1993.
- Moliner E., Museros P., and Martínez-Rodrigo M.D. Retrofit of existing railway bridges of short to medium spans for high-speed traffic using viscoelastic dampers. *Engineering Structures*, 40, 2012.
- Roy H., Dutt J., and Datta P. Dynamics of a viscoelastic rotor shaft using augmenting thermodynamic fields—a finite element. *International Journal of Mechanical Sciences*, 50:845–853, 2008.
- Saidi I., Gad E.F., Wilson J.L., and Haritos N. Development of passive viscoelastic damper to attenuate excessive floor vibrations. *Engineering Structures*, 33, 2011.
- Wang G., Veeramani S., and Wereley N. Analysis of sandwich plates with isotropic face plates and a viscoelastic core. *Journal of Vibration and Acoustics*, 112:305–312, 2000.
- Wang Y. and Inman D. Finite element analysis and experimental study on dynamic properties of a composite beam with viscoelastic damping. *Journal of Sound and Vibration*, 332:6177–6191, 2013.